

# SOLUTION OF THE GENERAL HELMHOLTZ EQUATION STARTING FROM LAPLACE'S EQUATION

**Tapan K. Sarkar and Young-seek Chung**

Department of Electrical Engineering and Computer Science  
121 Link Hall

Syracuse University

Syracuse, New York 13244-1240.

Phone: 315-443-3775, Fax: 315-443-4441.

Email: [tk Sarkar@syr.edu](mailto:tk Sarkar@syr.edu), Homepage: <http://web.syr.edu/~tk Sarkar>

**Magdalena Salazar Palma**

Grupo de Microondas y Radar, Dpto. Senales, Sistemas y Radiocomunicaciones

ETSI Telecomunicacion, Universidad Politecnica de Madrid

Ciudad Universitaria, 28040 Madrid, Spain.

E-mail: [salazar@gmr.ssr.upm.es](mailto:salazar@gmr.ssr.upm.es)

**ABSTRACT:** In this paper we illustrate how to solve the general Helmholtz equation starting from Laplace's equation. The interesting point is that the Helmholtz equation has a frequency term whereas Laplace's equation is the static solution of the same boundary value problem. In this new formulation the frequency dependence is manifested in the form of an excitation. A new boundary integral method for solving the general Helmholtz equation is developed. This new formulation is developed for the two-dimensional Helmholtz equation with the method of moments Laplacian solution. The main feature of this new formulation is that the boundary conditions are satisfied independent of the region node discretizations. The numerical solution of the present method is compared with finite difference and finite element solutions of the same problem. Application of this method is also presented for the computation of cut-off frequencies for some canonical waveguide structures.

## I. INTRODUCTION

The two dimensional Helmholtz's equation is an important equation to be solved in many numerical electromagnetics problems such as waveguide related problems and appears in a variety of physical phenomena and engineering applications, such as, acoustic radiation [1], heat conduction [2], and water wave propagation [3]. In semiconductor device modeling, Helmholtz's equation arises frequently as an intermediate step in the solution of the nonlinear Poisson's problem. To solve these problems diverse numerical methods have been reported which include finite difference [4], finite element [5], and boundary integral methods (BIM) [6-8]. Using these

conventional methods, it has been found that fine grids and a large number of elements must be employed to get satisfactory accuracy [3]. This requires large computer core storage, and more computational time especially for the iteration scheme of the nonlinear Poisson's problem where the value at each grid point needs to be updated at each step of the iteration. Further, the BIM formulations are in most cases limited to homogeneous Helmholtz equation and tied closely to the particular problem at hand [6]. In this paper, a simple approach to solve the homogeneous and nonhomogeneous Helmholtz equations is proposed. The technique is based on the computation of Laplacian potential by the method of moments (MoM) [9], without resorting to different formulations using Hankel functions as it is commonly done in BIM [10]. Besides its generality to solve Laplace's, Poisson's, and Helmholtz's equations in one single code implementation, the present method will considerably reduce the number of domain grids compared to the finite difference methods and does not require any interpolation. The accuracy of the MOM solution from this new formulation will be compared with the solutions of fine difference method (FDM) and finite element method (FEM), using the ELLPACK implementation [4].

## II. MATHEMATICAL FORMULATION

Consider the following two-dimensional elliptic equation for a smooth function  $\Psi$  defined in a 2-D region defined by  $\mathfrak{R}$  which is bounded by a contour  $C$  so that

$$\nabla^2 \Psi(x, y) + \lambda(x, y) \Psi(x, y) = F(x, y) \quad (1)$$

where  $\lambda$  and  $F$  are known functions in the domain  $\mathfrak{R}$ . The general form of (1) includes, as specializations, the following cases:

- 1) Laplace's equation, with  $\lambda = 0$  and  $F = 0$
- 2) Poisson's equation, with  $\lambda = 0$  and  $F \neq 0$ .
- 3) Helmholtz's equation, with  $\lambda \neq 0$  and  $F \neq 0$ .

So only one general formulation addresses the solution to all of the three cases above. In addition we illustrate how to use the frequency independent solution of the Laplace's equation to solve the general Helmholtz equation. On the contour  $C$  the boundary condition can be of Dirichlet, Neumann, or mixed type, as given by the general form

$$\alpha\Psi + \beta\frac{\partial\Psi}{\partial n} = \gamma \quad (2)$$

where  $\alpha$ ,  $\beta$ ,  $\gamma$ , are known spatial functions and  $\partial\Psi/\partial n$  represents the normal derivative. It is implied that a consistent set of boundary conditions has been chosen for the problem.

The proposed scheme to solve the given boundary value problem starts by assuming the term  $\lambda\Psi$  to be a known function, and including it with the given excitation function  $F$ , and thereby reducing (1) to the familiar Poisson's equation

$$\nabla^2\Psi(x, y) = -\Theta(x, y) \quad (3)$$

with

$$\Theta(x, y) = \lambda(x, y)\Psi(x, y) - F(x, y). \quad (4)$$

The solution to Poisson's equation in (3) can be expressed as

$$\Psi = \phi_h + \phi_p \quad (5)$$

where  $\phi_h$  is the solution to the homogeneous Poisson's equation (Laplace's equation)

$$\nabla^2\phi_h = 0 \quad (6)$$

and  $\phi_p$  is the particular integral, i.e.,

$$\nabla^2\phi_p = -\Theta(x, y) \quad (7)$$

Here we use the particular solution of the Poisson's equation given by [12]

$$\phi_p(x, y) =$$

$$\frac{1}{2\pi} \iint_{\mathfrak{R}} \Theta(x', y') \ln \left( \frac{K}{\sqrt{(x-x')^2 + (y-y')^2}} \right) dx' dy' \quad (8)$$

where the spatial sets  $(x, y)$  and  $(x', y')$  denote the spatial coordinates of the field and source coordinates, respectively, and  $K$  is an arbitrary constant. Here,  $\ln(K)$  represents the value of the scalar potential  $\phi$  at infinity for the two dimensional case. For the 3D case, this term does not exist, as the potential at infinity is zero. Hence the Green's function is simply  $1/R$  instead of the natural log function. The value of the parameter  $K$  is chosen to be 100 for the 2-D problem as the reference potential at infinity is not zero but finite.

An expression similar to (8) can be derived to approximate the Laplacian potential  $\phi_h$ . The potential  $\phi_h$  can be assumed to be produced by some equivalent sources consisting of electrical charges,  $\sigma$  located on the contour  $C$  [12]. Then the potential  $\phi_h$  at any point  $(x, y)$  can be obtained from  $\sigma(x, y)$  using the following integral [9]

$$\phi_h(x, y) =$$

$$\frac{1}{2\pi} \int_C \sigma(x', y') \ln \left( \frac{K}{\sqrt{(x-x')^2 + (y-y')^2}} \right) dl' \quad (9)$$

where  $l'$  is the arc length on the contour  $C$ .

The boundary condition of the homogeneous potential  $\phi_h$  is obtained from (2) and (5) as

$$\alpha\phi_h + \beta\frac{\partial\phi_h}{\partial n} = \gamma - \left( \alpha\phi_p + \beta\frac{\partial\phi_p}{\partial n} \right). \quad (10)$$

It can be seen that (6) along with the boundary condition of (10), constitute a similar boundary-value problem. A similar problem was addressed in [9] almost thirty years ago.

This completes the formulation of the problem. The characteristic features of this formulation are:

- a. The frequency term appears in an explicit form.
- b. The Green's function and the unknowns are independent of frequency. The Green's function is in fact the static Green's function.

Next we illustrate how to solve these coupled equations both for the homogeneous part and the particular integral.

### III. NUMERICAL SOLUTION USING THE METHOD OF MOMENTS (MOM)

In order to solve the above equations given by (8)-(10) we employ the Method of Moments.

To evaluate the above integral in (8) we divide the domain  $\mathfrak{R}$  into  $N$  sub-regions. The midpoint coordinates of each of the sub-regions  $\Delta\mathfrak{R}_i$  are denoted by  $(x_{2i}, y_{2i})$ . Then the potential  $\phi_p$  at the field point  $(x, y)$  is approximated by

$$\phi_p(x, y) \cong \sum_{i=1}^N \Theta(x_{2i}, y_{2i}) a_i(x, y) \quad (11)$$

where

$$a_i(x, y) =$$

$$\frac{1}{2\pi} \iint_{\Delta\mathfrak{R}_i} \ell n \left( \frac{K}{\sqrt{(x-x')^2 + (y-y')^2}} \right) dx' dy' \quad (12)$$

Hence it is assumed that  $\Theta(x, y)$  is constant within each sub-region  $\Delta\mathfrak{R}_i$  and is equal to the value  $\Theta(x_{2i}, y_{2i})$ .

Next we show how to numerically evaluate (9). Here, we take recourse to MOM. We expand the surface unknown  $\sigma$  using a pulse expansion. For purposes of illustration and simplicity let us choose point matching. Through the use of a pulse-expansion and point-matching techniques we will solve the present problem given by (9). Furthermore, if the contour  $C$  is segmented by  $M$  straight lines of length  $\Delta C_i$  between points  $i$  and  $i + 1$ , then  $\sigma$  can be represented by the step approximation

$$\sigma = \sum_{i=1}^M \sigma_i P_i(l) \quad (13)$$

where  $P_i(l)$  is a pulse function equal to 1 on  $\Delta C_i$  and zero elsewhere and  $\sigma_i$  is its unknown amplitude. Substituting (13) into (9), we obtain an approximation for  $\phi_h$

$$\phi_h(x, y) \cong \sum_{i=1}^M \sigma_i c_i(x, y) \quad (14)$$

where

$$c_i(x, y) = \int_{\Delta C_i} \ell n \left( \frac{K}{\sqrt{(x-x')^2 + (y-y')^2}} \right) dl' \quad (15)$$

Using (4), (11) and (14), the Helmholtz potential  $\Psi$  at an arbitrary field point  $(x, y)$  can now be expressed as

$$\Psi(x, y) = \sum_{i=1}^M \sigma_i c_i(x, y) + \sum_{i=1}^N (\lambda_i \Psi_i - F_i) a_i(x, y) \quad (16)$$

where for simplicity we have used the following abbreviations in (4):

$$\begin{aligned} \lambda_i &= \lambda(x_{2i}, y_{2i}) \\ F_i &= F(x_{2i}, y_{2i}) \\ \Psi_i &= \Psi(x_{2i}, y_{2i}) \end{aligned}$$

The unknown function  $\Psi(x, y)$  in (16) of Helmholtz equation can now be evaluated once the unknown terms,  $\sigma_i$  and  $\Psi_i$ , are determined. Next a system of two matrix equations is derived and solved for the unknowns  $\sigma_i$  and  $\Psi_i$ . The first matrix equation of this system is readily obtained by satisfying (16) at the midpoints  $(x_{2j}, y_{2j})$  of each of the  $N$  sub-region  $\Delta\mathfrak{R}_i$ . Using matrix notation, we obtain

$$[\Psi_i] = [p_{ji}] [\sigma_i] + [q_{ji}] [\lambda_i \Psi_i - F_i] \quad (17)$$

where  $p_{ji} = c_i(x_{2j}, y_{2j})$ , and  $q_{ji} = a_i(x_{2j}, y_{2j})$ .

The second matrix equation is now obtained by enforcing the boundary condition of (10) as follows. We define  $\hat{r}_j = (x_j, y_j)$ ,  $j = 1, 2, \dots, M$ , to be the midpoints of  $\Delta C_j$ . The boundary conditions are enforced at each  $\hat{r}_j$ . Substitution of (11) and (14) into (10) gives the following set of equations

$$\begin{aligned} \sum_{i=1}^M \sigma_i w_{ji} &= \lambda_j - \sum_{i=1}^N (\lambda_i \Psi_i - F_i) b_{ji} \\ j &= 1, 2, \dots, M \end{aligned} \quad (18)$$

where  $w_{ji} = \gamma(\hat{r}_j)$  and

$$w_{ji} = \left( \alpha c_i + \beta \frac{\partial c_i}{\partial n} \right)_{(x,y)=\hat{r}_j} \quad (19)$$

$$b_{ji} = \left( \alpha a_i + \beta \frac{\partial a_i}{\partial n} \right)_{(x,y)=\hat{r}_j} \quad (20)$$

Equation (18) can now be written in matrix notations as

$$[w_{ji}][\sigma_i] = [\gamma_j] - [b_{ji}][\lambda_i \Psi_i - F_i] \quad (21)$$

Observe that (17) and (21) form a system of two equations in two unknowns  $\sigma_i$  and  $\Psi_i$ , from which they can be solved. We use (21) to obtain an expression for  $\sigma$  and then substitute it into (17), and after simple matrix manipulations we obtain the following equation for  $\Psi_i$

$$[A][\Psi_i] = [B] \quad (22)$$

where

$$[A] = [I] + \left( [p_{ji}][w_{ji}]^{-1}[b_{ji}] - [q_{ji}] \right) [\lambda_i] \quad (23)$$

$$[B] = \left( [p_{ji}][w_{ji}]^{-1}[\gamma_j] + [p_{ji}] - [w_{ji}]^{-1}[b_{ji}] - [q_{ji}] \right) [F_i] \quad (24)$$

and  $[I]$  denotes the  $N \times N$  identity matrix.

From the last three equations some general comments can be made:

- 1) Analytic expressions can easily be derived for the evaluation of all the terms of the matrices  $[A]$  and  $[B]$  that include the integrals (12) and (15). This is true at least for the 2-D case.
- 2) The matrix elements  $[w_{ji}]$ , which are a part of the system matrix of the moment method, are similar to the matrix elements obtained in [9]. For different Helmholtz problems with different boundary conditions,  $[w_{ji}]$  remains unchanged. This observation is important in an iteration scheme where the boundary conditions are kept the same.
- 3) Problems with multiple right-hand sides are solvable with minimum additional computation time since the function  $F$  in (17) appears only as a term of matrix  $[B]$  in (24).
- 4) The domain and the contour discretization schemes are totally independent. This feature can offer the flexibility to handle boundary discontinuities without the need for excessive domain grid generations. This will be

illustrated through numerical examples in the next section.

- 5) Once  $\Psi_i$  is determined at the grid points, using Gaussian elimination for instance the potential at any other point is obtained using ordinary matrix multiplications as shown by (17). No interpolations are needed.

Next, we illustrate these points through some numerical examples.

### III. STATIC APPLICATIONS

*Example 1—Water Wave Propagation:* As a first example, we consider the problem of water wave propagation in a rectangular basin  $100\text{m} \times 100\text{m}$  [3]. Denoting by  $\Psi$  the water evaluation, then the wave propagation is governed by (1) with  $F = 0$ , and  $\lambda = k^2$  where  $k$  is the wave number. The boundary conditions used are displayed in Figure 1. The solution by MOM is compared to the solutions obtained by finite difference method (FDM) and finite element method (FEM) for various mesh sizes inside the domain. The minimum number of nodes required for each method to converge to the exact solution at any arbitrary point is optimized. Figure 2 compares the solutions computed along the line  $x = 90$  by the Method of Moments utilizing  $(1 \times 1)$ ,  $(2 \times 2)$  and  $(4 \times 4)$  grids. Figure 3 shows the solutions obtained by the finite element method utilizing  $(5 \times 5)$ ,  $(10 \times 10)$ , and  $(20 \times 20)$  grids. Figure 4 shows the results obtained by the finite difference method utilizing  $(5 \times 5)$ ,  $(15 \times 15)$ , and  $(35 \times 35)$  grids. In all these figures, the solid line represents the exact solution. Referring to these figures, one can easily observe that a considerably smaller number of nodes is employed with the present method than with the conventional methods. The minimum number of the domain nodes required to obtain a satisfactory accuracy using MOM for the present method is 16  $(4 \times 4)$ , compared to 400  $(20 \times 20)$  for FEM or up to 1000 nodes for FDM.

*Example 2—MOST Modeling:* The nonlinear Poisson's equation plays a key role in numerical modeling of semi-conductor devices. Many important characteristics of VLSI devices can be extracted from the solution of Poisson's equation. The most common approach to the numerical solution of the nonlinear Poisson's equation is based on the application of Newton's method to simultaneous discretized equations [15]. This approach often requires large storage especially for fine meshes, as is the case for two-dimensional modeling of the MOST [14].

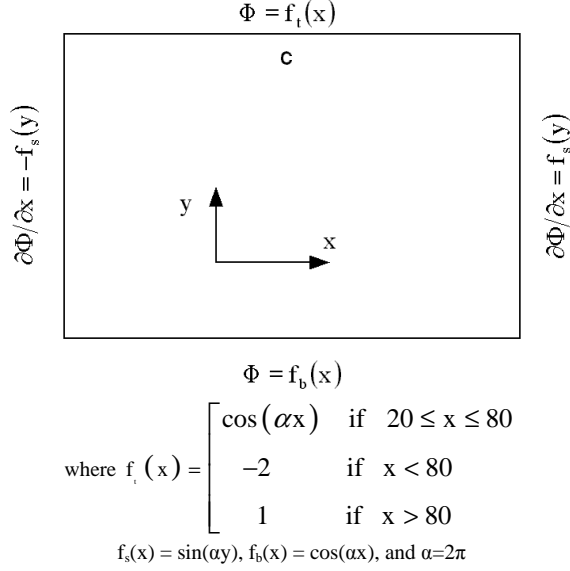


**Figure 1.** Physical structure and the associated boundary conditions associated with Example 1.

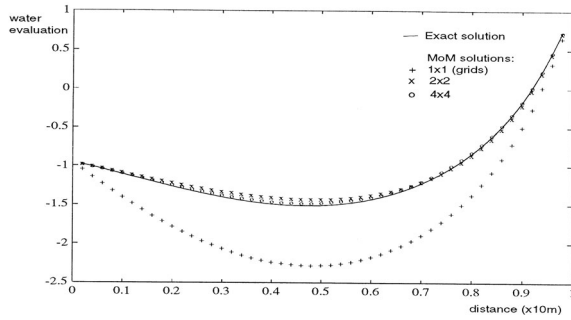


**Figure 2.** Solution obtained by the present method.

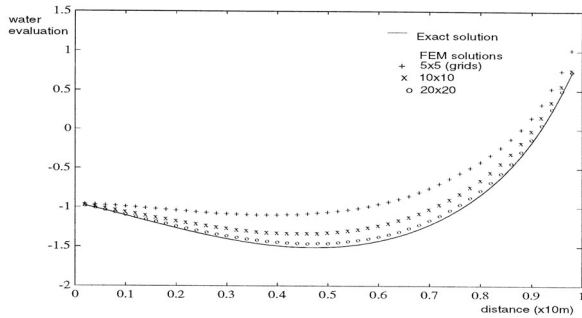


**Figure 3.** The FEM solution for Example 1.

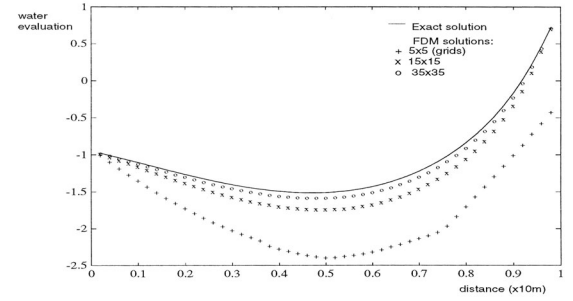


**Figure 4.** The FDM solution for Example 1.

In this section the MOM is applied to solve the nonlinear Poisson's equation that arises in the MOST modeling. We consider the MOST structure of Figure 5 made on a  $p$ -type substrate with doping  $N_A$ . Under the low current approximation the potential  $\Phi$  is governed by the Poisson's equation [16]

$$\frac{\partial^2 \Psi}{\partial x^2} + \frac{\partial^2 \Psi}{\partial y^2} = \frac{n_i}{L_D^2} \left( e^{-\Psi} - e^{\Psi} - \frac{N_A}{n_i} \right) \quad (25)$$

where  $\Psi = \Phi/V_T$  is the normalized potential,  $V_T$  is the thermal potential,  $n_i$  is the intrinsic carrier concentration, and  $L_D$  is the Debye length.

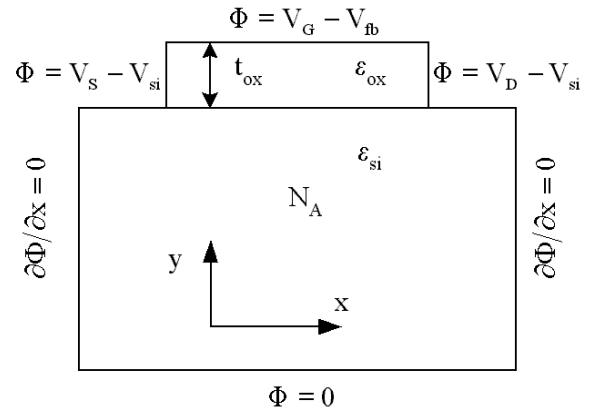


**Figure 5.** The physical structure and the associated boundary condition for MOST modeling.

The boundary conditions adopted along the edges of the device are the same as those used by [16], [12], and are displayed in Figure 5. On the oxide-semiconductor interface the following boundary condition is assumed

$$\epsilon_{ox} \frac{V_G - \Phi - V_{FB}}{t_{ox}} = \epsilon_s \frac{\partial \Phi}{\partial y} \quad (26)$$

where  $\epsilon_{ox}$ , and  $\epsilon_s$  are, respectively, the oxide and silicon permittivities,  $V_{FB}$  is the flat band voltage, and  $t_{ox}$  is the oxide thickness.

To solve the above elliptic problem we proceed first by dividing the boundary into  $M$  segments. Finer segments are used on the top edge of the device to handle its boundary discontinuities. Using the boundary conditions, and the technique described in [9], matrix  $[w_{ji}]$  is computed, then inverted and stored. Independently, the base region is also divided into  $N$  finite elements or cells. We seek to determine the electric potential at each midpoint of the cells using (25) which is nonlinear. To solve it we set up an iterative procedure, based on Newton's linearization [15]. At the  $k$ -th iteration we replace the right-hand side of (25) by its Fourier expansion about  $\Psi^k$ . Then the following Helmholtz's equation is obtained

$$\frac{\partial^2 \Psi^{(k+1)}}{\partial x^2} + \frac{\partial^2 \Psi^{(k+1)}}{\partial y^2} - G(\Psi^{(k)}) \Psi^{(k+1)} = F(\Psi^{(k)}) \quad (27)$$

where  $F$  and  $G$  are given by

$$F(\Psi^{(k)}) = \frac{n_i}{L_D^2} \left( (\Psi^{(k)} + 1) e^{-\Psi^{(k)}} + (\Psi^{(k)} - 1) e^{\Psi^{(k)}} - \frac{N_A}{n_i} \right) \quad (28)$$

$$G(\Psi^{(k)}) = \frac{n_i}{L_D^2} (e^{-\Psi^{(k)}} + e^{\Psi^{(k)}}) \quad (29)$$

The iteration scheme starts by taking some initial guess value for  $\Psi^{(0)}$  so that (27) can be solved for the first approximation  $\Psi^{(1)}$ . Then  $\Psi^{(1)}$  is used to find the second approximation  $\Psi^{(2)}$ . The procedure is repeated until the norm  $\| \Psi^{(k+1)} - \Psi^{(k)} \|$  is less than a desired tolerance. However, this iteration scheme often diverges [13], [15], and some damping factor was found necessary to improve the convergence of the iterative solution. At the beginning of the  $k$ -th iteration step, the following formula was used for all inner nodes

$$\Psi^{(k+1)} = (1-R)\Psi^{(k-1)} + R\Psi^{(k)} \quad (30)$$

where  $R (< 1)$  is the relaxation factor.

The accuracy of the solution obtained by the present technique is demonstrated by comparing it with the FDM (5-point) solution. For both methods, MOM and FDM, we let the values of the electric potential to be updated at each mesh point by means of an explicit formula, that is, without the solution of simultaneous algebraic equations [15]. We assign  $\Psi = 0$ , as an initial guess for all the inner nodes. Once the convergence is attained for the domain nodes, then the electric potential at any other point in the device is determined by a matrix multiplication as shown in (17), and without the need of any interpolation. For numerical computations, the following data were used: The thickness of the oxide layer was  $t_{ox} = 0.5 \mu\text{m}$ , the flat band voltage is  $V_{FB} = -1 \text{ V}$  and the doping profile is assumed to be uniform with  $N_A = 10^{18} \text{ cm}^{-3}$ ,  $n_i = 1.5 \times 10^{10} \text{ cm}^{-3}$ , thermal potential,  $V_T = 0.0258 \text{ V}$ , and  $R = 0.1$ . The results of the computations are shown in Figure 6, where the distribution of the electric potential at the thermal equilibrium is plotted along different lines parallel to the  $x$ -axis. The solid lines represent the solution obtained using the FDM and (o) symbol is reserved for the solutions obtained by the present method. Close agreements can be observed between the two methods. However, for FDM 721 nonuniform mesh points are employed to reduce the total number of nodes {for uniform meshes over 4900 (70×70) nodes ought to be used}. Finer meshes were chosen in the depletion region and near the junctions to reproduce accurately the fast variation of the electric potential [16] and the surface discontinuities of the potential; whereas for MOM, the number of the uniform meshes was 529 (23×23) or 400 for nonuniform cells. The number of iterations required for the convergence was 51 with the present technique as compared to 108 iterations with FDM to reach the point at which the absolute maximum between two subsequent iterations was less than 0.05 (tolerance).

Next we apply this method to the solution of the cutoff-frequencies of various waveguides.

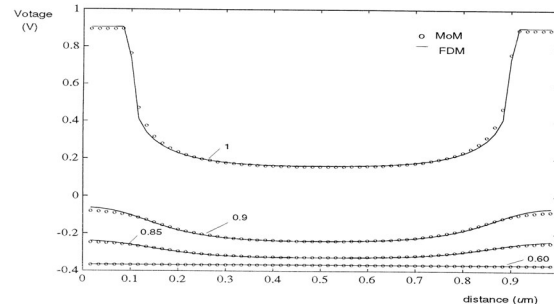


**Figure 6:** The distribution of the electric potentials along the lines parallel to the  $x$ -axis.

#### IV. SOLUTION OF THE GENERAL HELMHOLTZ EQUATION FOR HOMOGENEOUSLY FILLED WAVEGUIDES

In waveguides, solution of the Helmholtz equation determines the electromagnetic field configuration within the guides. It is convenient to divide the possible field configurations within the waveguides into two sets, namely TM waves and TE waves, each of which is governed by similar Helmholtz equations.

If we consider a waveguide in which the direction of propagation of the wave is along the  $z$ -direction, then the Helmholtz equations are as follows.

TM <sub>$z$</sub>  Case ( $H_z \equiv 0$ ):

$$\nabla^2 E_z(x, y) + (\omega^2 \mu \varepsilon - K_z^2) E_z(x, y) = 0 \quad (31)$$

with the appropriate boundary conditions  $E_z = 0$ , on the conductor walls and for the

TE <sub>$z$</sub>  Case ( $E_z \equiv 0$ ):

$$\nabla^2 H_z(x, y) + (\omega^2 \mu \varepsilon - K_z^2) H_z(x, y) = 0 \quad (32)$$

with appropriate boundary conditions  $\partial H_z / \partial n = 0$ , on the conductor walls where  $\partial H_z / \partial n$  represents the normal derivative. Here,

- $E_z$   $z$ -component of the electric field;
- $H_z$   $z$ -component of the magnetic field;
- $\omega$  angular frequency =  $2\pi f$ ;
- $f$  frequency of interest;
- $\mu$  permeability of the homogeneous medium;
- $\varepsilon$  permittivity of the homogeneous medium;
- $K_z$  propagation constant in the  $z$ -direction.

Comparing (31) and (32) with (1), and also the boundary conditions of the TM <sub>$z$</sub>  and TE <sub>$z$</sub>  cases with those of the general equations, we can draw the following analogies as outlined in Table I.

By examining (32) that

$$[B] = [p_{ji}] [w_{ji}]^{-1} [\gamma_j] + ([p_{ji}] [w_{ji}]^{-1} [b_{ji}] - [q_{ji}]) [F_i]$$

it can be inferred that  $[B] = 0$ , since  $F = 0$  and  $\gamma = 0$  for TM <sub>$z$</sub>  and TE <sub>$z$</sub>  cases.

In the case of TM <sub>$z$</sub> , (22) reduces to the form

$$[A] \cdot [E_{zi}] = 0 \quad (33)$$

In the case of TE <sub>$z$</sub> , (22) reduces to the form

$$[A] \cdot [H_{zi}] = 0 \quad (34)$$

Here again,  $E_{zi}$  and  $H_{zi}$  refer to the values of  $E_z$  and  $H_z$  at the midpoints of the subregions of the discretized waveguide cross section.

For (33) and (34), nontrivial solutions exist for  $[E_{zi}]$  and  $[H_{zi}]$  only if the matrix  $[A]$  is singular. The condition for nontrivial (i.e., nonzero) solutions to exist for  $[E_{zi}]$  and  $[H_{zi}]$  it is essential that

$$\det[A] = 0 \quad (35)$$

where  $\det[A]$  stands for *determinant of*  $[A]$ . We know from (23) that

$$[A] = ([p_{ji}] [w_{ji}]^{-1} [b_{ji}] - [q_{ji}]) [\lambda_i] + [I]$$

and we also know that for the cases of the TM <sub>$z$</sub>  and TE <sub>$z$</sub>  waves

$$\lambda = \omega^2 \mu \varepsilon - K_z^2. \quad (36)$$

**Table I**  
Special cases of the General Helmholtz Equation

General Equation (3)	TM <sub><math>z</math></sub> Equation (1)	TE <sub><math>z</math></sub> Equation (2)
$\nabla^2 \Psi + \lambda \Psi = F$	$\nabla^2 E_z + (\omega^2 \mu \varepsilon - K_z^2) \cdot E_z = 0$	$\nabla^2 H_z + (\omega^2 \mu \varepsilon - K_z^2) \cdot H_z = 0$
$\Psi$	$E_z$	$H_z$
$\lambda$	$\omega^2 \mu \varepsilon - K_z^2$	$\omega^2 \mu \varepsilon - K_z^2$
$F$	0	0
$\alpha \Psi + \beta \cdot \partial \Psi / \partial n = \gamma$	$E_z = 0$	$\partial H_z / \partial n = 0$
$\gamma$	0	0

Hence, given the frequency at which the Helmholtz equation is to be solved,  $\det [A]$  would be a function of  $K_z$ , the roots of which will provide the values of  $K_z$  for which  $\det [A] = 0$ . Once these  $K_z$  values are known, the eigenvector of  $[A]$  corresponding to the minimum eigenvalue gives the nontrivial solutions for  $[E_{zi}]$  and  $[H_{zi}]$  in case of  $TM_z$  and  $TE_z$  cases, respectively.

Once  $[E_{zi}]$  and  $[H_{zi}]$  are determined at the grid points, using Gaussian elimination for instance, the values of  $E_z$  and  $H_z$  at any other point can be obtained using ordinary matrix multiplications, as explained in [1].

#### IVa. Calculation of Propagation Constants for Different Waveguide Modes

It is evident that for the existence of nontrivial (nonzero) solutions for  $[E_{zi}]$  and  $[H_{zi}]$ , it is necessary that (35) be satisfied. Let us define a matrix  $[Z]$  such that

$$[Z] = ([p_{ji}][w_{ji}]^{-1}[b_{ji}] - [q_{ji}]). \quad (37)$$

Hence, (35) becomes

$$\det ([Z][\lambda_i] + [I]) = 0 \quad (38)$$

which can be rewritten as

$$\det \left( [Z] - \begin{pmatrix} -1 \\ \lambda_i \end{pmatrix} [I] \right) = 0. \quad (39)$$

Equation (39) is similar to the characteristic equation of matrix  $[Z]$ , with its eigenvalues given by  $-1/\lambda_i$ . Knowing that  $\lambda_i$  above  $\equiv \omega^2 \mu \epsilon - K_z^2$  for  $TM_z$  and  $TE_z$  cases, it can be concluded that

$$\frac{-1}{\lambda_i} = \frac{1}{(K_z^i)^2 - \omega^2 \mu \epsilon} = EV_i^{[Z]}, \quad (40)$$

$$i = 1, 2, \dots, N.$$

where  $K_z^i$  is the propagation constant of the  $i$ th mode and  $EV_i^{[Z]} \equiv$   $i$ th eigenvalue of  $[Z]$ .

Equation (40) can be rearranged as

$$(K_z^i)^2 = \omega^2 \mu \epsilon + \frac{1}{EV_i^{[Z]}}. \quad (41)$$

Therefore, the propagation constants of different modes in the waveguide are given by the following:

For  $(K_z^i)^2 > 0$ ,

$$K_z^i = \sqrt{\omega^2 \mu \epsilon + \frac{1}{EV_i^{[Z]}}} \quad \text{propagating modes} \quad (42)$$

For  $(K_z^i)^2 < 0$ ,

$$K_z^i = j \sqrt{\omega^2 \mu \epsilon - \frac{1}{EV_i^{[Z]}}} \quad \text{nonpropagating modes} \quad (43)$$

Results of propagation constants of various modes in a rectangular waveguide computed by this method are shown next.

#### IV b. Calculation of Cutoff Frequencies for Different Waveguide Modes

The cutoff frequencies for the various propagating modes in the waveguide are given by

$$f_c^i = \frac{v}{2\pi} \sqrt{(\omega^2 \mu \epsilon - (K_z^i)^2)} \quad (44)$$

where  $f_c^i \equiv$  cutoff frequency of the  $i$ th mode. Here,  $v \equiv$  velocity of light in the homogeneous medium  $\equiv 1/\sqrt{\mu \epsilon}$  and it can be deduced from (41) that

$$\omega^2 \mu \epsilon - (K_z^i)^2 = \frac{-1}{EV_i^{[Z]}}, \quad (45)$$

$$i = 1, 2, \dots, N$$

Using (45) in (44), we find the cutoff frequencies for the first  $N$  propagating modes as

$$f_c^i = \frac{v}{2\pi} \sqrt{\frac{-1}{EV_i^{[Z]}}}, \quad i = 1, 2, \dots, N. \quad (46)$$

The cutoff wave number  $k_c^i$  of the  $i$ th mode can be calculated from the cutoff frequency using the relation

$$k_c^i = \frac{2\pi f_c^i}{v}, \quad i = 1, 2, \dots, N$$

This method thereby provides a straightforward approach to find the cutoff frequencies (and, hence, cutoff wavenumbers) of any waveguide structure

without resorting to scanning over a wide range of frequencies, as is done in the Ritz-Galerkin and surface integral-equation methods.

### V a. Results: Rectangular Waveguide

Consider a rectangular waveguide. For the waveguide in Figure 7, the region was divided into 100 subregions and the boundary was discretized into 96 subcountours. The maximum matrix size involved in the computations was  $100 \times 100$ . Results have been displayed in Table II for the cutoff wave numbers of the first eight  $\text{TM}_z/\text{TE}_z$  modes. The computational time involved in finding the cutoff wavenumbers of the first 100 modes on a Sun SPARC 10 workstation was 16 s.

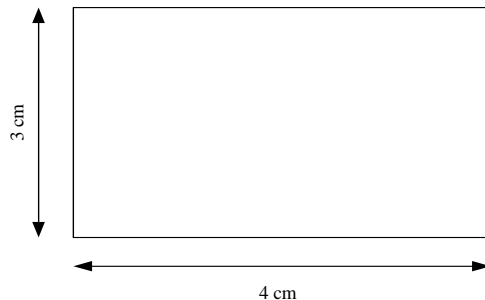


Figure 7. A rectangular waveguide.

Mode No.	Mode	$k_e$ actual (rad/cm)	$k_c$ computed (rad/cm)	Diff. %
1-0	$\text{TE}_z$	0.7857	0.7921	0.81
0-1	$\text{TE}_z$	1.0476	1.0536	0.57
1-1	$\text{TE}_z$ , $\text{TM}_z$	1.3095	1.3239	1.00
2-0	$\text{TE}_z$	1.5714	1.5827	0.72
2-1	$\text{TE}_z$ , $\text{TM}_z$	1.8886	1.9108	1.10
0-2	$\text{TE}_z$	2.0952	2.1095	0.68
1-2	$\text{TM}_z$ , $\text{TM}_z$	2.2377	2.2610	1.00
3-0	$\text{TE}_z$	2.3571	2.3896	1.30

### Vb. Single-Ridge Waveguide

A single ridge waveguide is a popular means of getting higher bandwidth. The first four  $\text{TM}_z$  and  $\text{TE}_z$  mode cutoff wavenumbers were computed for the single-ridge hollow waveguide shown in Figure 8. Results have been displayed in Table III and compared with published data. For the waveguide, the region

was divided into 96 subregions and the boundary was discretized into 112 subcountours. The maximum matrix size involved in computations was  $96 \times 96$ . The computational time involved in finding the cutoff wavenumbers of the first 96 modes in each case on a Sun SPARC 10 workstations was 18 s.

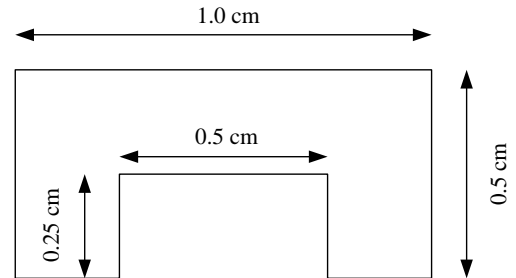


Figure 8. A single-ridge waveguide.

Mode No.	Mode	$k_c$ published (rad/cm)	$k_c$ computed (rad/cm)	Diff. %
1.	$\text{TM}_z$	12.1640 <sup>5</sup>	12.2338	0.57
2.	$\text{TM}_z$	12.2938 <sup>17</sup>	12.4106	0.95
3.	$\text{TM}_z$	13.9964 <sup>17</sup>	14.2152	1.56
4.	$\text{TM}_z$	15.5871 <sup>17</sup>	15.8221	1.50
5.	$\text{TE}_z$	2.2566 <sup>5</sup>	2.2688	0.54
6.	$\text{TE}_z$	4.9436 <sup>17</sup>	5.0149	1.44
7.	$\text{TE}_z$	6.5189 <sup>17</sup>	6.6289	1.68
8.	$\text{TE}_z$	7.5642 <sup>17</sup>	7.7097	1.92

## VI. CONCLUSION

An efficient technique based on MoM formulation for solving a general Helmholtz equation starting from Laplace's equation is presented. The main feature of this new formulation is that the boundary conditions are satisfied independent of the discretizations of the regions and the nodes. This feature was found especially useful when the boundary conditions have discontinuities. Considerable reduction in the domain grids is realized with the present method as compared to the conventional methods such as finite difference method or the finite element methods. In addition, one need not use a frequency dependent Green's function which can reduce the computational cost significantly.

## VII. REFERENCES

- [1] L. G. Copley, "Fundamental results concerning integral representation in acoustic radiation," *J. Acoust. Soc. Am.*, Vol. 44, pp. 28-32, 1963.

- [2] R. A. Altenkirch, M. Rezayat, R. Eichhorn, and F. J. Rizzo, "A study of heat conduction forward of flame in solids, by the boundary integral equation method," *Trans. ASME Ser. C. J. Heat Transfer*, Vol. 104, pp. 734–740, 1982.
- [3] M. Kawahara and K. Kashiya, "Boundary type finite element method for surface wave motion based on the trigonometric function interpolation," *Int. J. Numer. Meth. Eng.*, Vol. 21, pp. 1833–1852, 1985.
- [4] J. R. Rice and R. F. Boisvert, *Solving Elliptic Problems Using ELLPACK*. New York: Springer-Verlag, 1985.
- [5] P. L. Arlett, A. K. Bahrani, and O. C. Zienkiewicz, "Application of finite elements to the solution of Helmholtz's equation," *Proc. IEE*, Vol. 115, No. 12, pp. 1762–1766, 1968.
- [6] M. Rezayat, F. J. Rizzo, and D. J. Shippy, "A unified boundary integral equation method for class of second order elliptic boundary value problems," *J. Austral. Math. Soc. Ser.*, Vol. B–25, pp. 501–517, 1984.
- [7] K. Nagaya, and T. Yamaguchi, "Method for solving eigenvalue problems of the Helmholtz equation with an arbitrary shaped outer boundary and a number of eccentric inner boundaries of arbitrary shape," *J. Acoust. Soc. Am.*, Vol. 90, pp. 2146–2153, 1991.
- [8] P. J. Harris, "A boundary element method for Helmholtz equation using finite part integration," *Comp. Meth. Appl. Mech. Eng.*, Vol. 95, pp. 331–342, 1992.
- [9] R. F. Harrington, K. Pontoppidan, P. Abrahamsen, and N. C. Abertsen, "Computation of Laplacian potentials by an equivalent source method," *Proc. IEE*, Vol. 116, No. 10, pp. 1715–1920, 1969.
- [10] C. A. Brebbia, *The Boundary Element Method for Engineers*. New York: Wiley, 1978.
- [11] R. F. Harrington, *Field Computation by Moment Methods*. New York: Macmillan, 1968.
- [12] E. Arvas, R. I. Turkman, and P. S. Neelakantaswamy, "MOSFET analysis through numerical solution of Poisson's equation by the method of moments," *Solid-State Elect.*, Vol. 30, No. 12, pp. 1355–1361, 1987.
- [13] G. De Mey, "The boundary element method for modeling semiconductor components under low current approximation," in *Proc. Int. Conf. Simulation of Semiconductor Devices and Processes*, Pineridge Press, 1984, pp. 261–266.
- [14] W. Fichtner, D. J. Rose, and R. E. Bank, "Semiconductor device simulation," *IEEE Tran. Electron. Devices*, Vol. ED-30, No. 9, pp. 1018–1030, 1983.
- [15] W. F. Ames, *Nonlinear Partial Differential Equations in Engineering*. New York: Academic, 1965.
- [16] J. D. Kendall and A. R. Boothroyd, "A two-dimensional analytical threshold voltage model for MOSFET's with arbitrarily doped substrates," *IEEE Electron Device Lett.*, Vol. EDL–7, pp. 401–403, 1986.



**Tapan Kumar Sarkar**  
(<http://web.syr.edu/~tksarkar>)

received the B. Tech. degree from the Indian Institute of Technology, Kharagpur, India, in 1969, the M.Sc.E. degree from the University of New Brunswick, Fredericton, Canada, in 1971, and the M.S. and Ph.D. degrees from Syracuse University; Syracuse, New York in 1975.

From 1975 to 1976 he was with the TACO Division of the General Instruments Corporation. He was with the Rochester Institute of Technology, Rochester, NY, from 1976 to 1985. He was a Research Fellow at the Gordon McKay Laboratory, Harvard University, Cambridge, MA, from 1977 to 1978. He is now a Professor in the Department of Electrical and Computer Engineering, Syracuse University; Syracuse, NY. His current research interests deal with numerical solutions of operator equations arising in electromagnetics and signal processing with application to system design. He obtained one of the "best solution" awards in May 1977 at the Rome Air Development Center (RADC) Spectral Estimation Workshop. He has authored or coauthored ten books including the latest ones "Iterative and Self Adaptive Finite-Elements in Electromagnetic Modeling" and "Wavelet Applications in Engineering Electromagnetics" which were published in 1998 and 2002, respectively by Artech House, more than 210 journal articles and numerous conference papers and has written chapters in 28 books. The book on "Smart Antennas" will be published by John Wiley in March 2003.

Dr. Sarkar is a registered professional engineer in the State of New York. He received the Best Paper Award of the IEEE Transactions on Electromagnetic Compatibility in 1979 and in the 1997 National Radar Conference. He received the College of Engineering Research Award in 1996 and the chancellor's citation for excellence in research in 1998 at Syracuse University. He was elected Fellow of the IEEE in 1991. He was an Associate Editor for feature articles of the IEEE Antennas and Propagation Society Newsletter, and he was the Technical Program Chairman for the 1988 IEEE Antennas and Propagation Society International Symposium and URSI Radio Science Meeting.

Currently he is a distinguished lecturer for the IEEE Antennas and Propagation society. He is on the editorial board of Journal of Electromagnetic Waves and Applications and Microwave and Optical Technology Letters. He has been appointed U.S. Research Council Representative to many URSI General Assemblies. He was the Chairman of the Intercommission Working Group of International URSI on Time Domain Metrology (1990-1996). Dr. Sarkar is a member of Sigma Xi and International Union of Radio Science Commissions A and B. He received the title Docteur Honoris Causa from Universite Blaise Pascal, Clermont Ferrand, France in 1998 and the *Friends of Clermont Ferrand* award in 2000.



**Young-Seek Chung** received the B.S., M.S. and Ph.D. degrees in Electrical Engineering from Seoul National University, Seoul, Korea, in 1989, 1991, and 2000, respectively.

From 1991 to 1996, he was with the Living System Laboratory, LG Electronics. From 1998 to 2000, he was a Teaching Assistant in Electrical Engineering at the Seoul National University. Since 2001, he has been working at the Syracuse University with Dr. Tapan K. Sarkar. His current interests are the numerical analysis and the inverse scattering using the time domain techniques.



**Magdalena Salazar-Palma** was born in Granada, Spain. She received the degree of *Ingeniero de Telecomunicación* and the Ph.D. degree from the *Universidad Politécnica de Madrid* (Madrid, Spain), where she is a *Profesor Titular de Universidad* of the *Departamento de Señales, Sistemas y Radiocomunicaciones* (Signals, Systems and Radiocommunications Department) at the *Escuela Técnica Superior de Ingenieros de Telecomunicación* of the same university. She has taught courses on electromagnetic field theory, microwave and antenna theory, circuit networks and filter theory, analog and digital communication systems theory, numerical methods for electromagnetic field problems, as well as related laboratories.

She has developed her research within the *Grupo de Microondas y Radar* (Microwave and Radar Group) in the areas of electromagnetic field theory, computational and numerical methods for microwave structures, passive components, and antenna analysis; design, simulation, optimization, implementation, and measurements of hybrid and monolithic microwave

integrated circuits; and network and filter theory and design. For a number of times she has been a visiting professor at the Department of Electrical Engineering and Computer Science, Syracuse University (Syracuse, New York, USA).

She has authored three scientific books and a total of 15 contributions for chapters and articles in books published by international editorial companies, 25 papers in international journals, and 125 papers in international conferences, symposiums, and workshops, plus a number of national publications and reports. She has delivered a number of invited presentations, lectures, and seminars. She has lectured in several short courses, some of them in the frame of European Community Programs. She has participated in 45 projects and contracts, financed by international, European, and national institutions and companies. She has been a member of the Technical Program Committee of several international symposiums and has acted as reviewer for different international scientific journals, symposiums, and editorial companies. She has assisted the *Comisión Interministerial de Ciencia y Tecnología* (National Board of Research) in the evaluation of projects. She has also served in several evaluation panels of the Commission of the European Communities. In the past she has acted several times as topical editor for the disk of references of the triennial Review of Radio Science. She is a member of the editorial board of three scientific journals. She is a registered engineer in Spain. She is a senior member of the Institute of Electrical and Electronics Engineers (IEEE). She has served as vicechairman and chairman of IEEE Spain Section MTT-S/AP-S (Microwave Theory and Techniques Society / Antennas and Propagation Society) Joint Chapter and chairman of IEEE Spain Section. She is a member of IEEE Region 8 Nominations and Appointments Committee, IEEE Ethics and Member Conduct Committee, and IEEE Women in Engineering Committee (WIEC). She is acting as liaison between IEEE Regional Activities Board and IEEE WIEC. She has received two individual research awards from national institutions.